

X-Ray Crystallographic Studies on Fluxional Pentacoordinate Transition Metal Complexes. IV.¹⁻³ The Structure of (Norbornadiene)bis(dimethylphenylphosphine)-(trichlorostannato)iridium(I), (C₇H₉)(PMe₂Ph)₂Ir(SnCl₃), Including the Location and Refinement of All Hydrogen Atoms

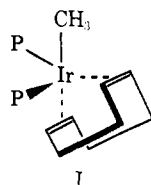
Melvyn Rowen Churchill* and Kuo-Kuang G. Lin

Contribution from the Department of Chemistry, University of Illinois at Chicago Circle, Chicago, Illinois 60680. Received July 26, 1973

Abstract: The fluxional pentacoordinate complex (norbornadiene)bis(dimethylphenylphosphine)(trichlorostannato)iridium(I), (C₇H₉)(PMe₂Ph)₂Ir(SnCl₃), crystallizes in the centrosymmetric monoclinic space group *P*₂₁/*c* [*C*₂^h; No. 14] with *a* = 9.616 (1) Å, *b* = 28.620 (6) Å, *c* = 9.764 (1) Å, and β = 96.72 (1)°. Observed and calculated densities are, respectively, 1.953 (10) and 1.958 g cm⁻³ for *Z* = 4 and *M* = 785.69. X-Ray diffraction data complete to 2θ = 50° (Mo Kα radiation) were collected with a Picker FACS-1 diffractometer, and the structure was solved using conventional Patterson, Fourier, and least-squares refinement techniques. All atoms (including hydrogens) were located, the final discrepancy indices being *R*_F = 3.93% and *R*_{wF} = 3.37% for the 4704 independent reflections. Bond distances around the iridium atom (in Å) are Ir-Sn = 2.5867 (6), Ir-P(1) = 2.306 (2), Ir-P(2) = 2.309 (2), Ir-olefin(A) = 2.068 (6), and Ir-olefin(B) = 2.123 (6) Å. The overall coordination geometry of the iridium atom is almost midway between trigonal bipyramidal (with P(1) and olefin(B) axial) and square pyramidal (with Sn axial), important angles (in deg) being Sn-Ir-P(1) = 95.79 (4), Sn-Ir-P(2) = 97.03 (4), Sn-Ir-A = 113.91 (17), Sn-Ir-B = 103.38 (16), P(1)-Ir-P(2) = 96.19 (5), P(1)-Ir-A = 93.86 (18), P(1)-Ir-B = 157.40 (16), P(2)-Ir-A = 146.25 (18), P(2)-Ir-B = 93.25 (18), and A-Ir-B = 67.57 (24). An interesting technical feature of the structural analysis is the successful location and refinement of all 30 hydrogen atoms in the presence of a third-row transition metal (*Z*(Ir) = 77) and other "heavy atoms" (*Z*(Sn) = 50, *Z*(Cl) = 17, *Z*(P) = 15); resulting C-H distances range from 0.81 (7) to 1.09 (6) Å (average = 0.965 Å).

We have previously reported the results of X-ray structural studies on the fluxional pentacoordinate (diolefin)bis(phosphine)methyliridium(I) species (C₈H₁₂)(PMe₂Ph)₂Ir(CH₃),¹ (C₈H₁₂)[Ph₂P(CH₂)₂-PPh₂Ir(CH₃)],² and (C₈H₁₂)[Ph₂P(CH₂)₃PPh₂Ir(CH₃)].³

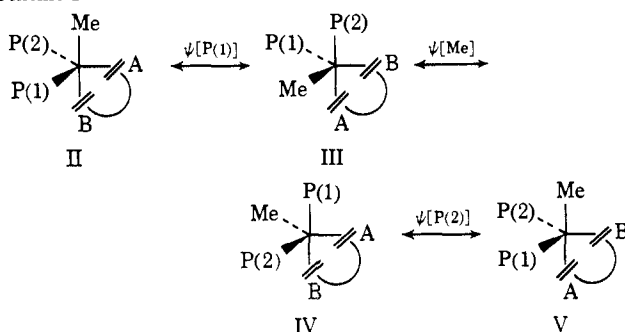
Two important results are forthcoming from these studies. (1) All three molecules have as their solid-state structure (and, also, as their ground state in solution^{4a}) a configuration which approximates to the trigonal bipyramidal geometry shown in I. The CH₃-



group, an excellent σ donor, occupies an axial site; the chelating cycloocta-1,5-diene ligand, which has a rather small "bite," is forced to span an axial and an equatorial position; and the two phosphine moieties occupy the remaining two equatorial positions. (2) For the (cycloocta-1,5-diene)bis(phosphine)methyliridium(I) species listed above, there is a relationship between the diequatorial P-Ir-P angle and the ease of intramolecular rearrangement in solution. In general, *omnia paribus*, the smaller the diequatorial P-Ir-P

angle, then the lower is the potential barrier to interconversion of isomers (as measured by the temperature at which, in solution, equilibration of the vinylic protons of the C₈H₁₂ ligand occurs). The suggested scheme^{4,5} for equilibration of these protons involves successive pseudorotations about P(1), Me, and P(2); see Scheme I. (Note that the rate-determining step is

Scheme I



II → III, which involves the transit of the methyl group into an energetically unfavorable equatorial position.)

Scheme I will not, however, be general to all (diolefin)bis(phosphine)iridium(X) species, because the ground-state geometry of such molecules is dependent upon the nature of X. When X is highly electronega-

(1) Part I: M. R. Churchill and S. A. Bezman, *Inorg. Chem.*, **11**, 2243 (1972).

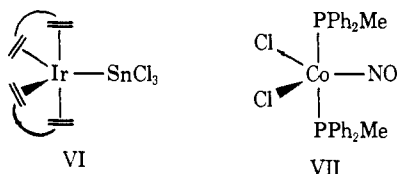
(2) Part II: M. R. Churchill and S. A. Bezman, *Inorg. Chem.*, **12**, 260 (1973).

(3) Part III: M. R. Churchill and S. A. Bezman, *Inorg. Chem.*, **12**, 531 (1973).

(4) (a) J. R. Shapley and J. A. Osborn, *J. Amer. Chem. Soc.*, **92**, 6976 (1970); (b) J. R. Shapley and J. A. Osborn, *Accounts Chem. Res.*, **6**, 305 (1973).

(5) It should be emphasized that the "turnstile mechanism" [see I. Ugi, D. Marquarding, H. Klusacek, P. Gillespie, and F. Ramirez, *Accounts Chem. Res.*, **4**, 288 (1971)] is permutationally indistinguishable from the Berry pseudorotation mechanism and can also explain the observed data. However, we refer the reader to the discussion of Shapley and Osborn (ref 4b, p 311): "...we prefer to describe the rearrangement in terms of the Berry [pseudorotation] mechanism rather than the turnstile, since the former is more evident to manipulate conceptually and easier to illustrate in practice."

tive or is a strong σ -donor, Scheme I may well be operative; if X is a strong π -acceptor ligand, Scheme I may well be invalid since X will tend preferentially to occupy an equatorial site, and species analogous to II and V will no longer represent the ground state. In keeping with this, $(C_8H_{12})_2Ir(SnCl_3)$ has been shown to have the structure VI^{6a} and $CoCl_2(NO)[PPh_2Me]_2$ has the structure VII;^{6b} *i.e.*, $SnCl_3^-$ and NO, two of the strongest



known π -acceptor ligands, occupy equatorial coordination positions.⁷

Shapley and Osborn have shown^{4b} that for complexes of the type (diolfin)bis(phosphine)Ir(SnCl₃) (which are prepared by the interaction of (diolfin)₂Ir(SnCl₃) and phosphine) replacement of two monodentate phosphine ligands by diphos (PPh₂P(CH₂)₂PPh₂) causes an increase in the barrier to intramolecular interconversion of isomers (*i.e.*, the chelate effect acts in precisely the opposite direction to that observed for methyliridium(I) species, *vide supra*).

We have now completed an X-ray diffraction study of (norbornadiene)bis(dimethylphenylphosphine)(trichlorostannato)iridium(I), $(C_7H_9)(PMe_2Ph)_2Ir(SnCl_3)$, with a view toward ascertaining the precise geometry of the iridium(I) coordination sphere and the relative orientation of ligands in the solid state (which we believe to be equivalent to the solution ground state). Our results are reported below.

Collection and Reduction of the X-Ray Diffraction Data

Yellow crystals of (norbornadiene)bis(dimethylphenylphosphine)(trichlorostannato)iridium(I), $(C_7H_9)(PMe_2Ph)_2Ir(SnCl_3)$, were provided by Mrs. S. A. Bezman and Professor J. A. Osborn of Harvard University.

The crystal selected for the structural analysis approximated in shape to a pentagonal prism extended along its *c* direction ($(001) \rightarrow (00\bar{1}) = 0.50$ mm). The prism faces (cyclically) were (110), $(\bar{1}\bar{1}0)$, $(0\bar{1}0)$, $(\bar{1}\bar{1}0)$, and $(\bar{1}10)$. The maximum thickness was 0.30 mm (from $(0\bar{1}0)$ to the intersection of (110) and $(\bar{1}\bar{1}0)$). Perpendicular to that direction the maximum thickness was 0.12 mm (from the intersection of (110) and $(\bar{1}\bar{1}0)$ to the intersection of $(\bar{1}\bar{1}0)$ and $(\bar{1}10)$).

Preliminary photographic data yielded approximate cell dimensions, revealed C_{2h} Laue symmetry for the crystal, and indicated the systematic absences $h0l$ for $l = 2n + 1$ and $0k0$ for $k = 2n + 1$, consistent only with the centrosymmetric monoclinic space group $P2_1/c$ [C_{2h}^2 ; No. 14].

The crystal was transferred to a Picker FACS-1 diffractometer,⁸

(6) (a) P. Porta, H. M. Powell, R. J. Mawby, and L. M. Venanzi, *J. Chem. Soc. A*, 455 (1967); (b) C. P. Brock, J. P. Collman, G. Dolcetti, P. H. Farnham, J. A. Ibers, J. E. Lester, and C. A. Reed, *Inorg. Chem.*, **12**, 1304 (1973).

(7) Our arguments concerning the preferential occupation of axial and equatorial sites are based on the following two (not necessarily mutually exclusive) assumptions: (i) that there are no large ligand-ligand interactions which will necessitate ligands occupying a specific site (*e.g.*, bulky ligands occupying equatorial sites—*cf.* ref 4b, p 310); (ii) that the pentacoordinate complex in question is able energetically to undergo intramolecular rearrangement. If the barrier to such a process is too high, then kinetic control (rather than thermodynamic control) may dictate the stereochemistry of the molecule. It might then be possible for various isomers to be isolated depending on the method of synthesis of the species. The reader will note that the examples given (VI and VII) are each fluxional molecules.

(8) Details of the apparatus and experimental procedure have been given previously; see M. R. Churchill and B. G. DeBoer, *Inorg. Chem.*, **12**, 525 (1973).

was centered, and was accurately aligned with its c^* axis coincident with the diffractometer's ϕ axis.

Unit cell parameters, obtained by a least-squares analysis of the 2θ , ω , and χ settings of the Mo $K\alpha_1$ component (λ 0.70926 Å) of 12 automatically centered reflections taken at 22° are $a = 9.6158$ (13), $b = 28.620$ (6), $c = 9.7644$ (14) Å, and $\cos \beta = -0.11704$ (20), corresponding to $\beta = 96.72$ (1) $^\circ$. The unit cell volume is 2668.8 Å³. The observed density, by flotation in aqueous BaI₂, is 1.953 (10) g cm⁻³. The density calculated for $M = 785.69$ and $Z = 4$ is 1.958 g cm⁻³. No crystallographic symmetry is imposed upon the molecule.

Intensity data were collected with Nb-filtered Mo $K\alpha$ radiation using a coupled θ (crystal): 2θ (counter) scan from 0.6° in 2θ below the $K\alpha_1$ peak to 0.6° in 2θ above the $K\alpha_2$ peak, thereby accumulating P counts in t_P seconds. The scan-rate was 1.0 deg min⁻¹, and stationary background counts, of 20-sec duration each, were collected at the low- and high- 2θ limits of the scan, yielding B_1 and B_2 counts, respectively, in a total background-counting time of $t_B = 40$ sec. Copper-foil attenuators, which reduced the intensity of the diffracted beam by successive (accurately known) factors of ~ 3.2 , were inserted when necessary to keep the counting rate below $\sim 10,000$ counts per second, thereby minimizing coincidence losses. The takeoff angle was 3.0° ; the scintillation counter was ~ 33 cm from the crystal and had an aperture of 6×6 mm.

Before collecting the data set, the intensity of the axial 002 reflection was measured by a θ - 2θ scan at $\chi = 90^\circ$ and at 10° intervals from $\phi = 0^\circ$ to $\phi = 350^\circ$. The maximum deviation from the mean was $\sim 40\%$, indicating that an absorption correction was mandatory.

All reflections of the type hkl and $h\bar{k}l$ in the angular range $0^\circ < 2\theta < 50^\circ$ were measured. Three strong "check reflections" (014, 080, 200) were measured after each batch of 48 reflections in order to monitor the stability of the entire assembly (*i.e.*, crystal stability, crystal alignment, electronic stability of apparatus, etc.). Root-mean-square deviations in the net intensities of the check reflections⁹ were 1.41, 1.82, and 1.70%, respectively.

A total of 4704 independent reflections (excluding systematic absences) were collected.

The integrated intensity, I , and its estimated standard deviation, $\sigma(I)$, were calculated *via* the expressions

$$I = q[(P + 4.5) - (t_P/t_B)(B_1 + B_2 + 9.0)]$$

and

$$\sigma(I) = q[(P + 4.5) + (t_P/t_B)^2(B_1 + B_2 + 9.0) + 24.75 + q^{-2}p^2I^2]^{1/2}$$

The "ignorance factor" (p) was set equal to 0.04, q represents the correction for attenuator used, and all numerical terms are introduced to allow for the fact that the last digit of each count (P , B_1 , B_2) is truncated during the output process.

Any negative I was reset to zero and was retained; *no data were rejected on the basis of not being significantly above background*.

Unscaled structure factor amplitudes, F , and their estimated standard deviations, $\sigma(F)$, were calculated as

$$F = (I/Lp)^{1/2}$$

$$\sigma(F) = [F_o - (F_o^2 - \sigma(I)/Lp)^{1/2}]$$

for $\sigma(I) < I$ and

$$\sigma(F) = (\sigma(I)/Lp)^{1/2}$$

for $\sigma(I) > I$. The Lorentz-polarization factor, Lp , is $(1 + \cos^2 2\theta)/(2 \sin 2\theta)$. All data were corrected for absorption ($\mu(\text{Mo } K\alpha) = 66.58 \text{ cm}^{-1}$), using the program DRAB;¹⁰ maximum and minimum transmission factors were 0.603 and 0.298. (Data from the axial reflection 002 (*vide supra*) were processed also; the corrected intensities were no longer significantly ϕ dependent, thereby providing an independent check on the validity of the absorption correction.)

Solution and Refinement of the Structure. Computer programs used in determining and refining the structure were FORDAP (Fourier synthesis, by A. Zalkin), SFIX (full-matrix least-squares refinement,

(9) All data analysis and data reduction processes were performed using the Fortran IV program RDUS by B. G. DeBoer.

(10) DRAB is a Fortran IV program for calculating absorption corrections written by B. G. DeBoer.

Table I. Atomic Coordinates and Isotropic Thermal Parameters, with Esd's, for $(C_7H_8)(PMe_2Ph)_2Ir(SnCl_3)^{a,b}$

Atom	x	y	z	B, Å ²
Ir	0.277662 (22)	0.109874 (6)	0.186163 (19)	2.25
Sn	0.165301 (43)	0.120366 (12)	-0.065853 (35)	2.86
Cl(1)	0.09016 (22)	0.19461 (6)	-0.16680 (17)	6.14
Cl(2)	0.29436 (23)	0.09759 (7)	-0.25220 (17)	6.93
Cl(3)	-0.04958 (26)	0.08171 (9)	-0.14510 (18)	8.80
P(1)	0.09895 (16)	0.14534 (5)	0.28568 (14)	2.69
P(2)	0.42214 (16)	0.17450 (5)	0.19431 (15)	3.18
C(1)	0.42551 (69)	0.03611 (20)	0.33903 (61)	3.93
C(2)	0.47598 (64)	0.06995 (19)	0.23236 (62)	3.57
C(3)	0.41313 (68)	0.05508 (20)	0.10420 (63)	3.77
C(4)	0.32269 (74)	0.01297 (20)	0.13450 (69)	4.18
C(5)	0.20941 (70)	0.03746 (19)	0.20446 (70)	3.88
C(6)	0.27543 (68)	0.05252 (20)	0.33269 (61)	3.75
C(7)	0.41158 (81)	-0.00930 (23)	0.25721 (79)	4.69
C(11)	-0.02676 (57)	0.10169 (18)	0.33181 (54)	2.93
C(12)	-0.03386 (68)	0.08859 (22)	0.46790 (57)	3.74
C(13)	-0.11884 (78)	0.05153 (23)	0.49599 (64)	4.58
C(14)	-0.19567 (69)	0.02761 (24)	0.39326 (68)	4.35
C(15)	-0.19021 (65)	0.04064 (23)	0.25847 (64)	4.07
C(16)	-0.10704 (63)	0.07794 (20)	0.22754 (58)	3.45
C(17)	-0.01429 (73)	0.18691 (22)	0.18420 (67)	3.92
C(18)	0.14920 (79)	0.17757 (21)	0.44365 (61)	3.87
C(21)	0.54181 (63)	0.18245 (20)	0.35332 (62)	3.83
C(22)	0.64927 (74)	0.21588 (25)	0.36093 (79)	5.02
C(23)	0.74323 (82)	0.21967 (31)	0.47740 (99)	6.41
C(24)	0.73493 (87)	0.19097 (30)	0.58762 (97)	6.55
C(25)	0.62771 (92)	0.15937 (29)	0.58467 (75)	6.15
C(26)	0.53139 (78)	0.15507 (23)	0.46771 (71)	4.65
C(27)	0.54370 (94)	0.17024 (29)	0.06550 (81)	5.59
C(28)	0.35059 (87)	0.23304 (23)	0.15869 (84)	5.19
H(1)	0.4681 (68)	0.0381 (20)	0.4334 (62)	5.4 (13)
H(2)	0.5665 (66)	0.0900 (20)	0.2467 (58)	5.1 (13)
H(3)	0.4399 (63)	0.0610 (19)	0.0162 (58)	4.7 (13)
H(4)	0.2916 (75)	-0.0028 (22)	0.0682 (67)	5.9 (16)
H(5)	0.1276 (74)	0.0302 (22)	0.1890 (66)	5.7 (13)
H(6)	0.2307 (50)	0.0611 (15)	0.4162 (45)	2.8 (15)
H(7A)	0.3532 (91)	-0.0313 (28)	0.3118 (80)	8.5 (21)
H(7B)	0.4933 (76)	-0.0198 (23)	0.2324 (66)	6.0 (18)
H(12)	0.0183 (69)	0.1027 (20)	0.5383 (63)	5.4 (15)
H(13)	-0.1291 (59)	0.0479 (17)	0.5870 (56)	4.3 (12)
H(14)	-0.2566 (56)	0.0017 (16)	0.4127 (50)	3.5 (10)
H(15)	-0.2491 (59)	0.0226 (19)	0.1865 (53)	4.3 (11)
H(16)	-0.0919 (66)	0.0875 (20)	0.1364 (61)	5.2 (12)
H(17A)	0.0527 (67)	0.2107 (20)	0.1546 (58)	5.1 (14)
H(17B)	-0.0658 (99)	0.1714 (30)	0.1086 (98)	10.6 (27)
H(17C)	-0.0868 (98)	0.1992 (30)	0.2399 (88)	9.6 (29)
H(18A)	0.0553 (88)	0.1917 (26)	0.4808 (74)	7.8 (20)
H(18B)	0.1894 (72)	0.1556 (23)	0.4932 (66)	6.0 (19)
H(18C)	0.2154 (65)	0.2045 (20)	0.4226 (57)	4.8 (13)
H(22)	0.6370 (96)	0.2425 (27)	0.2914 (78)	8.3 (20)
H(23)	0.8220 (80)	0.2428 (24)	0.4781 (68)	6.5 (15)
H(24)	0.7961 (93)	0.1877 (30)	0.6749 (82)	9.2 (22)
H(25)	0.6162 (72)	0.1375 (22)	0.6741 (69)	6.2 (16)
H(26)	0.4652 (71)	0.1373 (22)	0.4674 (63)	5.4 (11)
H(27A)	0.5014 (96)	0.1726 (29)	-0.0267 (89)	9.2 (24)
H(27B)	0.6044 (73)	0.1946 (22)	0.0592 (63)	5.5 (13)
H(27C)	0.6153 (77)	0.1450 (25)	0.0951 (67)	6.5 (26)
H(28A)	0.3060 (99)	0.2397 (30)	0.2393 (95)	8.1 (22)
H(28B)	0.4286 (83)	0.2540 (24)	0.1584 (69)	6.6 (17)
H(28C)	0.2891 (77)	0.2344 (22)	0.0611 (67)	6.0 (22)

^a Esd's (estimated standard deviations) are right adjusted to the last digit of the preceding number and are those derived from the inverse of the least-squares matrix. ^b For nonhydrogen atoms, the "equivalent isotropic thermal parameters" are listed. They correspond to the average of the mean-square displacements along the three principal axes of the anisotropic thermal ellipsoid.

derived from SFLS5, by C. T. Prewitt), STAN1 (distances and angles, with estimated standard deviations, by B. G. DeBoer), PLOD (least-squares planes, etc., by B. G. DeBoer), and ORTEP (thermal ellipsoid drawings, by C. K. Johnson). All calculations were performed on an IBM 370/155 computer at the University of Illinois at Chicago Circle.

Scattering factors for neutral Ir, Sn, Cl, P, and C were taken from the compilation of Cromer and Waber;¹¹ the real and imaginary

components of anomalous dispersion, taken from the table of Cromer and Liberman,¹² were included for all nonhydrogen atoms. Scattering factors for hydrogen atoms are those of Mason and Robertson.¹³

The function minimized in least-squares refinement processes was $\sum w(|F_o| - |F_c|)^2$; discrepancy indices used below are

$$R_F = \frac{\sum ||F_o| - |F_c||}{\sum |F_o|}$$

(12) D. T. Cromer and D. Liberman, *J. Chem. Phys.*, **53**, 1891 (1970).

(13) R. Mason and G. B. Robertson, *Advan. Struct. Res. Diffraction Methods*, **2**, 57 (1966).

(11) D. T. Cromer and J. T. Waber, *Acta Crystallogr.*, **18**, 104 (1965).

Table II. Anisotropic Thermal Parameters with Esd's^{a,b} for Nonhydrogen Atoms in the (C₇H₈)₂(PMe₂Ph)₂Ir(SnCl₃) Molecule

Atom	B ₁₁	B ₂₂	B ₃₃	B ₁₂	B ₁₃	B ₂₃	$\langle U \rangle^c$
Ir	2.39 (1)	2.18 (1)	2.12 (1)	0.11 (1)	-0.02 (1)	0.28 (1)	(0.150, 0.173, 0.182)
Sn	3.56 (2)	2.82 (2)	2.10 (2)	0.03 (1)	-0.12 (1)	0.19 (1)	(0.158, 0.190, 0.218)
Cl(1)	8.32 (12)	4.80 (7)	5.07 (8)	1.41 (7)	-0.24 (8)	1.22 (6)	(0.204, 0.279, 0.338)
Cl(2)	8.20 (12)	8.71 (11)	4.01 (7)	3.32 (10)	1.28 (8)	0.38 (7)	(0.220, 0.256, 0.386)
Cl(3)	9.42 (15)	12.19 (16)	4.48 (8)	-6.32 (13)	-0.48 (9)	-0.46 (9)	(0.208, 0.266, 0.469)
P(1)	2.91 (6)	2.68 (5)	2.44 (5)	0.27 (5)	0.14 (5)	0.01 (4)	(0.173, 0.180, 0.199)
P(2)	3.13 (7)	2.93 (6)	3.38 (7)	-0.38 (5)	0.04 (5)	0.45 (5)	(0.180, 0.193, 0.226)
C(1)	4.43 (32)	3.81 (26)	3.42 (26)	1.52 (23)	-0.04 (24)	0.95 (20)	(0.16, 0.23, 0.27)
C(2)	2.96 (27)	3.24 (24)	4.48 (28)	0.87 (20)	0.25 (23)	0.69 (20)	(0.16, 0.22, 0.25)
C(3)	3.91 (30)	4.13 (27)	3.36 (26)	0.96 (33)	0.85 (23)	0.27 (21)	(0.19, 0.20, 0.25)
C(4)	4.76 (34)	2.95 (24)	4.62 (30)	0.67 (22)	-0.37 (26)	-0.83 (21)	(0.18, 0.22, 0.28)
C(5)	3.54 (29)	2.28 (22)	5.79 (34)	0.04 (20)	0.51 (26)	0.60 (21)	(0.17, 0.21, 0.27)
C(6)	4.30 (30)	3.56 (25)	3.54 (26)	0.93 (22)	1.14 (23)	1.53 (20)	(0.16, 0.21, 0.27)
C(7)	4.22 (34)	3.91 (28)	5.88 (35)	1.13 (24)	0.34 (27)	0.86 (24)	(0.19, 0.25, 0.28)
C(11)	2.52 (23)	3.27 (23)	3.06 (23)	0.36 (18)	0.59 (19)	-0.25 (18)	(0.17, 0.20, 0.21)
C(12)	3.92 (30)	4.60 (28)	2.64 (23)	-0.48 (23)	0.04 (21)	-0.25 (20)	(0.18, 0.22, 0.25)
C(13)	5.28 (36)	5.55 (33)	2.92 (26)	-0.02 (27)	0.49 (26)	0.62 (22)	(0.19, 0.24, 0.29)
C(14)	3.46 (30)	4.97 (31)	4.61 (30)	-0.63 (24)	0.47 (25)	0.53 (24)	(0.20, 0.23, 0.26)
C(15)	2.93 (26)	5.24 (32)	3.93 (29)	-0.43 (23)	0.07 (23)	-0.34 (23)	(0.19, 0.23, 0.26)
C(16)	3.08 (26)	4.40 (27)	2.87 (24)	-0.32 (21)	0.36 (21)	-0.06 (20)	(0.19, 0.20, 0.24)
C(17)	3.95 (33)	3.69 (28)	4.09 (31)	0.82 (25)	0.29 (27)	0.59 (23)	(0.19, 0.23, 0.24)
C(18)	5.48 (37)	2.79 (26)	3.31 (27)	-0.02 (25)	0.32 (26)	-0.50 (21)	(0.18, 0.21, 0.26)
C(21)	3.15 (28)	3.81 (27)	4.37 (30)	0.06 (22)	-0.15 (24)	-0.64 (22)	(0.19, 0.21, 0.25)
C(22)	3.52 (32)	5.19 (34)	6.34 (38)	-0.69 (26)	0.50 (29)	-1.66 (28)	(0.20, 0.24, 0.31)
C(23)	3.62 (34)	7.24 (42)	8.23 (48)	-0.68 (31)	0.05 (34)	-3.89 (37)	(0.19, 0.24, 0.38)
C(24)	4.99 (39)	6.92 (41)	7.09 (44)	1.25 (33)	-2.09 (35)	-3.76 (35)	(0.19, 0.24, 0.40)
C(25)	6.63 (46)	6.82 (42)	4.48 (33)	1.21 (36)	-1.55 (33)	-1.75 (30)	(0.20, 0.27, 0.35)
C(26)	4.51 (35)	4.43 (30)	4.69 (30)	-0.12 (26)	-0.81 (27)	-0.68 (24)	(0.20, 0.24, 0.28)
C(27)	5.61 (44)	6.29 (44)	5.02 (41)	-2.29 (39)	1.30 (36)	0.38 (33)	(0.20, 0.26, 0.32)
C(28)	5.01 (39)	3.45 (27)	6.73 (45)	-0.97 (26)	-0.95 (35)	1.60 (27)	(0.19, 0.23, 0.33)

^a These anisotropic thermal parameters are analogous to the usual form of the isotropic thermal parameter and have units of Å². They enter the expression for the structure factor in the form: $\exp[-0.25(B_{11}h^2a^{*2} + B_{22}k^2b^{*2} + B_{33}l^2c^{*2} + 2B_{12}hka^*b^* + 2B_{13}hla^*c^* + 2B_{23}klb^*c^*)]$. ^b Esd's were obtained from the last cycle in which thermal parameters for the atom being considered were refined. ^c These values correspond to the root-mean-square amplitudes of vibration (in Å) of the atom along the three principal axes (minor, median, major, respectively) of its vibration ellipsoid. For relative orientations, see figures.

and

$$R_{wF} = [\sum w(|F_o| - |F_c|)^2 / \sum w|F_o|^2]^{1/2}$$

The positions of the iridium and tin atoms were found from a three-dimensional Patterson map. All other nonhydrogen atoms were found from subsequent electron density syntheses. Refinement of all atomic positional parameters, anisotropic thermal parameters for Ir, Sn, Cl, and P atoms, and isotropic thermal parameters for C atoms led to convergence with $R_F = 5.2\%$ and $R_{wF} = 5.4\%$. A difference-Fourier synthesis at this stage provided evidence for anisotropic motion of the carbon atoms and also revealed unequivocally the positions of 29 of the 30 hydrogen atoms (the position of H(28A) was not uniquely defined), with peak heights ranging from 0.55 to 0.95 e Å⁻³.

Refinement was continued, now using anisotropic thermal parameters for all nonhydrogen atoms and with all 30 hydrogen atoms included in calculated positions with $d(C-H) = 0.95$ Å¹⁴ and isotropic thermal parameters equal to those of their attached carbons. Two complete¹⁵ cycles of refinement led to convergence at the reduced discrepancy indices $R_F = 4.2\%$ and $R_{wF} = 4.0\%$.

At this stage we decided to test the feasibility of refining the positional and isotropic thermal parameters of the 30 hydrogen atoms. Two further complete cycles of refinement (using two blocks, as there were now 391 variables) led to convergence with $R_F = 3.98\%$ and $R_{wF} = 3.39\%$. Finally, all thermal parameters were held constant while the positional parameters for the 60 atoms were subjected to two cycles of full-matrix refinement. The final discrepancy indices were $R_F = 3.93\%$ and $R_{wF} = 3.37\%$. The correlation matrix from the final cycle of refinement was used in calculating estimated standard deviations on interatomic distances and angles.

The standard deviation in an observation of unit weight, defined

(14) M. R. Churchill, *Inorg. Chem.*, **12**, 1213 (1973).

(15) The large number of variable parameters (nine for each of the 30 nonhydrogen atoms, plus a scale factor—271 parameters in all) led to our refining the structure in two blocks, rather than using a full-matrix refinement.

by $[\sum w(|F_o| - |F_c|)^2 / (m - n)]^{1/2}$ was 0.95. The number of reflections (m) was 4704 and the total number of refined parameters (n) was 391, yielding an $m:n$ ratio of 12.0:1. The function $\sum w(|F_o| - |F_c|)^2$ was not appreciably dependent on either θ or on $|F_o|$, thereby indicating a correctly chosen weighting scheme.

The correctness and completeness of the structural analysis was confirmed by a final difference-Fourier synthesis on which the highest feature was a peak of 0.8 e Å⁻³ close to the iridium position.

A table of observed and calculated structure factor amplitudes is available.¹⁶ Positional and isotropic thermal parameters are listed in Table I; anisotropic thermal parameters are collected in Table II.

Description of the Molecular Structure

Interatomic distances and their estimated standard deviations (esd's) are shown in Table III; interatomic angles (with esd's) are given in Table IV. The overall molecular geometry, including the labeling of atoms and the positions of all hydrogen atoms, is illustrated in Figure 1. The individual molecules of (C₇H₈)₂(PMe₂Ph)₂Ir(SnCl₃) are mutually separated by normal van der Waals' distances; there are no abnormally short intermolecular contacts.

The Iridium(I) Coordination Sphere. The (norbornadiene)₂P₂Ir(SnCl₃) portion of the molecule is shown in Figure 2. This diagram perhaps overemphasizes the (only approximate) trigonal bipyramidal coordination environment of the iridium(I) atom, in which P(1) and the olefinic C(2)-C(3) bond are assigned to axial positions. A careful consideration of the bond angles around the iridium(I) atom shows that (with allowance

(16) See paragraph at end of paper regarding supplementary material.

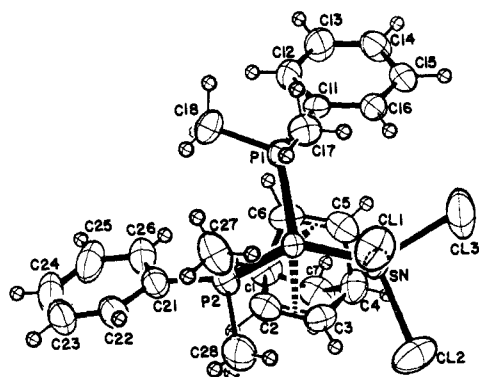


Figure 1. A general view of the $(C_7H_8)(PMe_2Ph)_2Ir(SnCl_3)$ molecule. (ORTEP diagram, showing 50% probability ellipsoids for nonhydrogen atoms and artificial 0.1 Å radius spheres for the hydrogen atoms.)

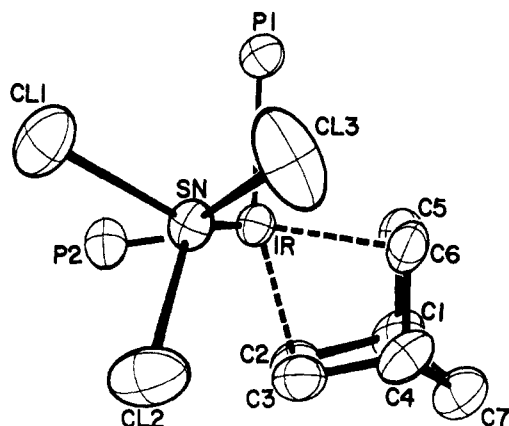


Figure 2. The immediate coordination sphere of the iridium atom. This diagram is orientated so as to emphasize the relationship of the coordination geometry to a regular trigonal bipyramidal arrangement.

being made for the ligand-enforced angle $A-Ir-B$,¹⁷ which is only 67.57 (24°) the overall coordination geometry of the iridium(I) atom is midway between trigonal bipyramidal (with P(1) and olefin(B)¹⁷ axial) and square pyramidal (with $SnCl_3$ axial), interligand angles being $Sn-Ir-P(1) = 95.79$ (4), $Sn-Ir-P(2) = 97.03$ (4), $Sn-Ir-A$ ¹⁷ = 113.91 (17), $Sn-Ir-B$ ¹⁷ = 103.38 (16), $P(1)-Ir-P(2) = 96.19$ (5), $P(1)-Ir-A = 93.86$ (18), $P(1)-Ir-B = 157.40$ (16), $P(2)-Ir-A = 146.25$ (18), and $P(2)-Ir-B = 93.25$ (18) $^\circ$.

However, for the convenience of subsequent discussions we will use the parlance of trigonal bipyramidal coordination geometry and refer to P(1) and the olefin C(2)-C(3) as "axial" ligands.

The iridium-phosphine distances are equivalent with $Ir-P = 2.3062$ (15) and $Ir-P(2) = 2.3090$ (15) Å. Similar values are found in other pentacoordinate iridium(I) species, *viz.*, 2.316 (5) and 2.329 (5) Å in $(C_8H_{12})(PMe_2Ph)_2Ir(CH_3)$,¹ 2.308 (3) Å in $(C_8H_{12})[Ph_2P(CH_2)_2PPh_2]Ir(CH_3)$,² and 2.309 (4) and 2.337 (4) Å in $(C_8H_{12})[Ph_2P(CH_2)_3PPh_2]Ir(CH_3)$.³ The "axial" olefinic linkage is more distant than the "equatorial" olefin, individual values being $Ir \cdots B$ (axial) = 2.123 (6) Å and $Ir \cdots A$ (equatorial) = 2.068 (6) Å. A similar pattern has emerged from our previous studies on (diolefin)bis-

(17) A is the midpoint of C(5)-C(6) and B is the mid point of C(2)-C(3).

Table III. Interatomic Distance (in Å) and Estimated Standard Deviations for $(C_7H_8)(PMe_2Ph)_2Ir(SnCl_3)$

Atoms	Distance	Atoms	Distance
(a) Distances around Iridium Atom			
Ir-Sn	2.5867 (6)	Ir-C(2)	2.224 (6)
Ir-P(1)	2.3062 (15)	Ir-C(3)	2.245 (6)
Ir-P(2)	2.3090 (15)	Ir-C(5)	2.188 (6)
Ir \cdots A ^a	2.068 (6)	Ir-C(6)	2.179 (5)
Ir \cdots B ^a	2.123 (6)		
(b) Distances around Tin Atom			
Sn-Cl(1)	2.417 (2)	Sn-Cl(3)	2.391 (3)
Sn-Cl(2)	2.409 (2)		
(c) Distances around Phosphorus Atoms			
P(1)-C(11)	1.831 (5)	P(2)-C(21)	1.835 (6)
P(1)-C(17)	1.825 (6)	P(2)-C(27)	1.819 (9)
P(1)-C(18)	1.814 (6)	P(2)-C(28)	1.829 (7)
		Av	1.826
(d) Carbon-Carbon Distances within Norbornadiene Ligand			
C(1)-C(2)	1.542 (8)	C(6)-C(1)	1.512 (9)
C(2)-C(3)	1.391 (9)	C(7)-C(1)	1.523 (9)
C(3)-C(4)	1.535 (9)	C(7)-C(4)	1.527 (10)
C(4)-C(5)	1.523 (9)		
C(5)-C(6)	1.404 (9)		
(e) Carbon-Carbon Distances in Phenyl Rings			
C(11)-C(12)	1.390 (8)	C(21)-C(22)	1.404 (9)
C(12)-C(13)	1.386 (9)	C(22)-C(23)	1.372 (12)
C(13)-C(14)	1.359 (9)	C(23)-C(24)	1.364 (12)
C(14)-C(15)	1.375 (9)	C(24)-C(25)	1.369 (12)
C(15)-C(16)	1.388 (9)	C(25)-C(26)	1.389 (11)
C(16)-C(11)	1.382 (8)	C(26)-C(21)	1.378 (9)
		Av	1.380 ± 0.013^b
(f) Carbon-Hydrogen Distances in Norbornadiene Ligand			
C(1)-H(1)	0.96 (6)	C(5)-H(5)	0.81 (7)
C(2)-H(2)	1.04 (6)	C(6)-H(6)	1.00 (4)
C(3)-H(3)	0.94 (6)	C(7)-H(7A)	1.03 (8)
C(4)-H(4)	0.82 (6)	C(7)-H(7B)	0.90 (7)
		Av	0.94 ± 0.09^b
(g) Carbon-Hydrogen Distances in Phenyl Ring			
C(12)-H(12)	0.90 (6)	C(22)-H(22)	1.02 (8)
C(13)-H(13)	0.91 (5)	C(23)-H(23)	1.00 (7)
C(14)-H(14)	0.98 (5)	C(24)-H(24)	0.98 (8)
C(15)-H(15)	0.99 (5)	C(25)-H(25)	1.09 (6)
C(16)-H(16)	0.96 (6)	C(26)-H(26)	0.82 (7)
		Av	0.97 ± 0.07^b
(h) Carbon-Hydrogen Distances in Methyl Groups			
C(17)-H(17A)	1.00 (6)	C(27)-H(27A)	0.95 (9)
C(17)-H(17B)	0.95 (9)	C(27)-H(27B)	0.92 (7)
C(17)-H(17C)	1.00 (9)	C(27)-H(27C)	1.02 (7)
C(18)-H(18A)	1.09 (8)	C(28)-H(28A)	0.96 (9)
C(18)-H(18B)	0.86 (6)	C(28)-H(28B)	0.96 (8)
C(18)-H(18C)	1.03 (6)	C(28)-H(28C)	1.06 (7)
		Av	0.98 ± 0.06^b

^a A is the midpoint of C(5)-C(6) and B is the midpoint of C(2)-C(3). ^b The number following " \pm " is the root-mean-square scatter (*i.e.*, an external estimate of the error on an individual bond length) and is calculated *via* the expression rms scatter = $[\sum(\chi_i - \bar{\chi})^2 / (N - 1)]^{1/2}$ where χ_i is the *i*th and $\bar{\chi}$ is the mean of *N* "equivalent" bond lengths, and the sum is over all *N* observations.

(phosphine)methyliridium(I) species: individual values for $Ir \cdots$ olefin (axial) and $Ir \cdots$ olefin (equatorial) in these complexes are, respectively, 2.117 (14) and 2.078 (14) Å in $(C_8H_{12})(PMe_2Ph)_2Ir(CH_3)$,¹ 2.106 (9) and 2.011 (9) Å in $(C_8H_{12})[Ph_2P(CH_2)_2PPh_2]Ir(CH_3)$,² and 2.127 (12) and 2.033 (12) Å in $(C_8H_{12})[Ph_2P(CH_2)_3PPh_2]Ir(CH_3)$.³ The statistical significance of the difference, calculated using $\sigma(\text{diff}) = (\sigma_1^2 + \sigma_2^2)^{1/2}$, is

Table IV. Bond Angles (in deg) with Esd's, for $(C_7H_8)(PMe_2Ph)_2Ir(SnCl_3)$

Atoms	Angle	Atoms	Angle
(A) Angles around Iridium Atom			
Sn-Ir-P(1)	95.79 (4)	P(1)-Ir-A ^a	93.86 (18)
Sn-Ir-P(2)	97.03 (4)	P(1)-Ir-B ^a	157.40 (16)
Sn-Ir-A ^a	113.91 (17)	P(2)-Ir-A ^a	146.25 (18)
Sn-Ir-B ^a	103.38 (16)	P(2)-Ir-B ^a	93.25 (18)
P(1)-Ir-P(2)	96.19 (5)	A-Ir-B ^a	67.57 (24)
(B) Angles around Tin Atom			
Ir-Sn-Cl(1)	124.17 (4)	Cl(1)-Sn-Cl(2)	94.92 (7)
Ir-Sn-Cl(2)	119.50 (5)	Cl(1)-Sn-Cl(3)	93.96 (8)
Ir-Sn-Cl(3)	120.20 (5)	Cl(2)-Sn-Cl(3)	97.60 (7)
(C) Angles around Phosphorus Atoms			
Ir-P(1)-C(11)	110.44 (17)	Ir-P(2)-C(21)	116.33 (20)
Ir-P(1)-C(17)	119.01 (22)	Ir-P(2)-C(27)	110.81 (27)
Ir-P(1)-C(18)	116.41 (25)	Ir-P(2)-C(28)	121.05 (26)
C(11)-P(1)-C(17)	102.08 (29)	C(21)-P(2)-C(27)	101.73 (34)
C(11)-P(1)-C(18)	104.81 (28)	C(21)-P(2)-C(28)	103.41 (32)
C(17)-P(1)-C(18)	102.30 (30)	C(27)-P(2)-C(28)	100.83 (37)
(D) C-C-C Angles within C ₇ H ₈ Ligand			
C(2)-C(1)-C(6)	98.7 (4)	C(3)-C(4)-C(5)	100.2 (5)
C(2)-C(1)-C(7)	101.4 (5)	C(3)-C(4)-C(7)	101.6 (5)
C(6)-C(1)-C(7)	102.6 (6)	C(5)-C(4)-C(7)	101.8 (5)
C(1)-C(2)-C(3)	106.1 (5)	C(4)-C(5)-C(6)	105.6 (6)
C(2)-C(3)-C(4)	105.3 (5)	C(5)-C(6)-C(1)	105.7 (5)
		C(1)-C(7)-C(4)	93.6 (5)
(E) C-C-C and P-C-C Angles within PMe ₂ Ph Ligands			
C(16)-C(11)-C(12)	119.1 (5)	C(26)-C(21)-C(22)	117.9 (6)
C(11)-C(12)-C(13)	119.5 (5)	C(21)-C(22)-C(23)	120.5 (7)
C(12)-C(13)-C(14)	121.4 (6)	C(22)-C(23)-C(24)	120.9 (8)
C(13)-C(14)-C(15)	119.5 (6)	C(23)-C(24)-C(25)	119.7 (8)
C(14)-C(15)-C(16)	120.3 (6)	C(24)-C(25)-C(26)	120.3 (8)
C(15)-C(16)-C(11)	120.3 (5)	C(25)-C(26)-C(21)	120.8 (7)
P(1)-C(11)-C(12)	121.8 (4)	P(2)-C(21)-C(22)	120.9 (5)
P(1)-C(11)-C(16)	118.8 (4)	P(2)-C(21)-C(26)	121.2 (5)
(F) C-C-H and H-C-H Angles in C ₇ H ₈ Ligand			
C(2)-C(1)-H(1)	118 (4)	C(4)-C(5)-H(5)	122 (5)
C(6)-C(1)-H(1)	108 (4)	C(6)-C(5)-H(5)	125 (4)
C(7)-C(1)-H(1)	124 (4)	C(5)-C(6)-H(6)	128 (3)
C(1)-C(2)-H(2)	126 (3)	C(1)-C(6)-H(6)	123 (3)
C(3)-C(2)-H(2)	124 (3)	C(1)-C(7)-H(7A)	106 (5)
C(2)-C(3)-H(3)	129 (4)	C(1)-C(7)-H(7B)	114 (4)
C(4)-C(3)-H(3)	123 (4)	C(4)-C(7)-H(7A)	112 (5)
C(3)-C(4)-H(4)	116 (5)	C(4)-C(7)-H(7B)	111 (4)
C(5)-C(4)-H(4)	113 (5)	H(7A)-C(7)-H(7B)	119 (7)
C(7)-C(4)-H(4)	121 (5)		
(G) C-C-H Angles in Phenyl Rings			
C(11)-C(12)-H(12)	122 (4)	C(21)-C(22)-H(22)	117 (5)
C(13)-C(12)-H(12)	119 (4)	C(23)-C(22)-H(22)	121 (5)
C(12)-C(13)-H(13)	114 (3)	C(22)-C(23)-H(23)	119 (4)
C(14)-C(13)-H(13)	123 (4)	C(24)-C(23)-H(23)	120 (4)
C(13)-C(14)-H(14)	122 (3)	C(23)-C(24)-H(24)	131 (5)
C(15)-C(14)-H(14)	119 (3)	C(25)-C(24)-H(24)	109 (5)
C(14)-C(15)-H(15)	117 (3)	C(24)-C(25)-H(25)	121 (4)
C(16)-C(15)-H(15)	123 (3)	C(26)-C(25)-H(25)	119 (4)
C(15)-C(16)-H(16)	125 (4)	C(25)-C(26)-H(26)	120 (5)
C(11)-C(16)-H(16)	114 (4)	C(21)-C(26)-H(26)	119 (5)
(H) P-C-H and H-C-H Angles in Methyl Groups			
P(1)-C(17)-H(17A)	104 (4)	H(17A)-C(17)-H(17B)	113 (7)
P(1)-C(17)-H(17B)	110 (5)	H(17A)-C(17)-H(17C)	116 (6)
P(1)-C(17)-H(17C)	110 (5)	H(17B)-C(17)-H(17C)	105 (8)
P(1)-C(18)-H(18A)	109 (4)	H(18A)-C(18)-H(18B)	115 (6)
P(1)-C(18)-H(18B)	100 (5)	H(18A)-C(18)-H(18C)	110 (5)
P(1)-C(18)-H(18C)	109 (3)	H(18B)-C(18)-H(18C)	114 (6)
P(2)-C(27)-H(27A)	114 (6)	H(27A)-C(27)-H(27B)	95 (7)
P(2)-C(27)-H(27B)	118 (4)	H(27A)-C(27)-H(27C)	121 (7)
P(2)-C(27)-H(27C)	109 (4)	H(27B)-C(27)-H(27C)	98 (6)
P(2)-C(28)-H(28A)	103 (6)	H(28A)-C(28)-H(28B)	108 (6)
P(2)-C(28)-H(28B)	107 (4)	H(28A)-C(28)-H(28C)	118 (6)
P(2)-C(28)-H(28C)	111 (3)	H(28B)-C(28)-H(28C)	109 (6)

^a A is the center of C(5)-C(6) and B is the center of C(2)-C(3).

6.5 σ for (C₇H₈)(PMe₂Ph)₂Ir(SnCl₃), 2.0 σ for (C₈H₁₂)-(PMe₂Ph)₂Ir(CH₃),¹ 7.5 σ for (C₈H₁₂)[Ph₂P(CH₂)₂PPh₂Ir-(CH₃),² and 5.5 σ for (C₈H₁₂)[Ph₂P(CH₂)₃PPh₂Ir(CH₃).³ A similar pattern is also observed^{6a} in bis(cycloocta-1,5-diene)(trichlorostannato)iridium(I), (C₈H₁₂)₂Ir-(SnCl₃); in this trigonal bipyramidal species, the Ir...olefin (axial) distances are 2.135 (26) and 2.134 (24) Å while the Ir...olefin (equatorial) distances are shorter at 2.068 (31) and 2.053 (34) Å.

The equatorial iridium-tin bond length of 2.5867 (6) Å may be compared to the analogous distance of 2.642 (2) Å for the equatorial Ir-SnCl₃ linkage in (C₈H₁₂)₂Ir(SnCl₃).^{6a} Each of these distances is shorter than the value of 2.75 Å suggested^{6a} for an iridium-tin linkage of unit bond order; this may be taken as indicative of multiple bond character in these Ir-SnCl₃ linkages.

Within the framework of the trigonal bipyramidal description of the structure, the equatorial plane defined by Sn, P(2), and A (the midpoint of the olefinic linkage, C(5)-C(6)), is described by the equation 0.7918X - 0.4644Y - 0.3967Z = -0.0282 (see Table V). The

Table V. Least-Squares Planes within the (C₇H₈)(PMe₂Ph)₂Ir(SnCl₃) Molecule^{a-c}

Atom	Dev, Å	Atom	Dev, Å
Plane I: 0.7918X - 0.4644Y - 0.3967Z = -0.0282			
Sn*	0.000	Ir	-0.203
P(2)*	0.000	P(1)	-2.507
A*	0.000	C(2)	+1.619
C(5)	+0.153	C(3)	+1.947
C(6)	-0.153	B	+1.782
Plane II: 0.7732X - 0.6316Y - 0.0568Z = -2.5221			
C(11)*	+0.009	C(14)*	+0.004
C(12)*	-0.002	C(15)*	+0.003
C(13)*	-0.004	C(16)*	-0.009
Plane III: -0.6350X + 0.6778Y + 0.3706Z = 1.7748			
C(21)*	-0.017	C(24)*	-0.019
C(22)*	+0.008	C(25)*	+0.009
C(23)*	+0.011	C(26)*	+0.009

^a Planes are in Cartesian coordinates such that [X,Y,Z] = [xa + zc cos β, yb, zc sin β]. ^b Planes are derived using unit weights for atoms marked with an asterisk and zero weight for all other atoms. ^c A is the midpoint of C(5)-C(6) and B is the midpoint of C(2)-C(3).

iridium atom is displaced from this plane (by 0.203 Å) in the direction of atom P(1), which itself lies 2.507 Å above (relative to Figure 2) the equatorial coordination plane. The olefinic linkage does not lie parallel with this plane but is canted such that atom C(5) is displaced by +0.153 Å and atom C(6) by -0.153 Å from the equatorial plane. Atoms of the axial olefinic ligand, C(2)-C(3), are similarly asymmetrically situated with respect to the equatorial coordination plane of the trigonal bipyramidal, with C(2) lying 1.619 and C(3) lying 1.947 below this plane.

The Phosphine Ligands. The phosphorus-phenyl bond distances are P(1)-C(11) = 1.831 (5) Å and P(2)-C(21) = 1.835 (6) Å, while phosphorus-methyl distances range from 1.814 (6) to 1.829 (7) Å (averaging 1.822 Å). The C-P-C angles range from C(27)-P(2)-C(28) = 100.83 (37)° to C(11)-P(1)-C(18) = 104.81 (28)°, the mean of the six independent values being 102.53°. This result is, however, characteristic both of metal-phosphine complexes and of free phosphines

and has previously been noted by Churchill and O'Brien.¹⁸ To our knowledge not even qualitative correlations have been discovered between deviations of C-P-C angles from the regular tetrahedral value and properties (or absence) of a metal-phosphine linkage. The Ir-P-C angles in the present complex range from 110.44 (17) to 121.05 (26)°, the mean being 115.66°.

As shown in Table V, the two phenyl rings are planar within the limits of experimental error; root-mean-square deviations from planarity are 0.006 Å for plane II (defined by C(11) through C(16)) and 0.014 Å for plane III (defined by C(21) through C(26)).

Individual carbon-carbon distances range from 1.359 (9) to 1.390 (8) Å in the phenyl group attached to P(1) and from 1.364 (12) to 1.404 (9) Å within the phenyl group attached to P(2); the mean of the 12 independent measurements is 1.380 Å, which may be compared to the accepted C-C(aromatic) distance of 1.394 ± 0.005 Å.¹⁹ C-C-C angles within the two phenyl groups range from 119.1 (5) to 121.4 (6)° and from 117.9 (6) to 120.9 (8)°; the mean of the 12 values is 120.0°, as expected for a planar hexagon. Interestingly, in each case the smallest angle is that associated with the P-bonded carbon atom, *i.e.*, C(16)-C(11)-C(12) = 119.1 (5)° and C(26)-C(21)-C(22) = 117.9 (6)°.

Carbon-hydrogen distances range from 0.90 (6) to 0.99 (5) Å in the C(11)-C(16) phenyl ring and 0.82 (7) to 1.09 (6) Å in the C(21)-C(26) ring. The average value of 0.97 Å is contracted by 0.11 Å from the recognized *internuclear* carbon-hydrogen distance of 1.08 Å; this effect is due to the centroid of the electron density around the hydrogen atom not being coincident with the nuclear position and has been discussed previously.²⁰

The C-C-H angles within the phenyl rings range from 109 (5) to 131 (5)°; however, all but these two extreme values are within 6° (approximately 1.5 σ) of the ideal external bisecting angle of 120° for a regular, planar hexagon. The positions of the phenyl hydrogen atoms are thus chemically sensible and provide justification for our refinement of atomic parameters for these atoms.

Within the four methyl groups, carbon-hydrogen distances range from 0.86 (6) to 1.09 (8) Å, the mean of the 12 independent values being 0.98 Å. The P-C-H angles range from 100 (5) to 118 (4)° (average = 108.7°), while H-C-H angles vary from 95 (7) to 121 (7)° (average = 110.2°). While variations in these angles are large, it must be emphasized that *in no case* does an angle deviate from the ideal tetrahedral value of 109.5° by more than ~2 σ .

The SnCl₃ Group. Individual tin-chlorine distances are 2.417 (2), 2.409 (2), and 2.391 (3) Å (average = 2.406 Å). Similar values (*i.e.*, 2.406 (12), 2.395 (8), 2.384 (10) Å; mean = 2.395 Å) were found within the (C₈H₁₂)₂Ir(SnCl₃) molecule.^{6a} However, in each case the reported distances may well be systematically reduced from their true value by libration of the SnCl₃ moiety about the Ir-Sn axis. (As shown clearly in Figure 2, the thermal ellipsoid for the tin(IV) atom approximates to spherical whereas those for the chlorine

(18) M. R. Churchill and T. A. O'Brien, *J. Chem. Soc. A*, 2970 (1968); see, especially, Table 7 on p 2976.

(19) L. E. Sutton, Ed., *Chem. Soc., Spec. Publ., No. 18*, S16s (1965).

(20) R. F. Stewart, E. R. Davidson, and W. T. Simpson, *J. Chem. Phys.*, **42**, 3175 (1965); see also ref 14.

atoms show pronounced elongation in a direction tangential to an imaginary circle drawn through Cl(1), Cl(2), and Cl(3).) Nevertheless, the observed tin-chlorine distances are all substantially longer than the value of $2.31 \pm 0.015 \text{ \AA}$ found in SnCl_4 .²¹

The coordination geometry of the tin(IV) atom is severely distorted from that of an idealized tetrahedron. Thus, the Ir-Sn-Cl angles are each more than 10° greater than the ideal tetrahedral angle of 109.47° , with Ir-Sn-Cl(1) = $124.17 (4)^\circ$, Ir-Sn-Cl(2) = $119.50 (5)^\circ$, and Ir-Sn-Cl(3) = $120.20 (5)^\circ$ (average = 121.29°). The Cl-Sn-Cl angles are correspondingly reduced from 109.47° , by more than 10° in each case, with Cl(1)-Sn-Cl(2) = $94.92 (7)^\circ$, Cl(1)-Sn-Cl(3) = $93.96 (8)^\circ$, and Cl(2)-Sn-Cl(3) = $97.60 (7)^\circ$ (average = 95.49°).

This pattern appears to be general for M-SnX_3 systems (M = transition metal, X = halogen). Thus, in $(\pi\text{-C}_5\text{H}_5)\text{Fe}(\text{CO})_2(\text{SnCl}_3)$ ²² Fe-Sn-Cl = $121.2 (1)$, $120.0 (1)$, and $116.3 (1)^\circ$ (average, 119.2°) and Cl-Sn-Cl = $100.2 (1)$, $98.6 (1)$, and $96.1 (1)^\circ$ (average, 98.3°); in $(\pi\text{-C}_5\text{H}_5)\text{Fe}(\text{CO})_2(\text{SnBr}_3)$ ²³ Fe-Sn-Br = $118.4 (1)$, $117.6 (1)$, and $117.0 (1)^\circ$ (average, 117.7°) and Br-Sn-Br = $101.6 (1)$, $100.3 (1)$, and $98.6 (1)^\circ$ (average, 100.2°); and in $(\text{C}_8\text{H}_{12})_2\text{Ir}(\text{SnCl}_3)$ ^{6a} Ir-Sn-Cl = $125.3 (3)$, $123.3 (2)$, and $113.5 (2)^\circ$ (average, 120.7°) and Cl-Sn-Cl = $96.8 (3)$, $95.7 (4)$, and $95.4 (4)^\circ$ (average, 96.0°). Distortions in the same direction but of lesser magnitude are commonly found in M-SiX_3 complexes²⁴ and in M-SnR_3 (R = alkyl or aryl group) species²⁵⁻²⁹ and appear to be characteristic of group IVB ligands bonded to transition metals.³⁰ The direction of these distortions is in accordance with Bent's rules.³¹

The Norbornadiene Ligand. The norbornadiene ligand behaves as a chelating diolefin and has a normal geometry. The coordinated double bonds C(2)-C(3) and C(5)-C(6) are, respectively, $1.391 (9)$ and $1.409 (9) \text{ \AA}$ in length. The mean value of 1.400 \AA is significantly (*i.e.*, $\sim 7\sigma$) greater than the recognized uncoordinated C=C distance of $1.335 \pm 0.005 \text{ \AA}$.¹⁹ Previous X-ray crystallographic studies of norbornadiene complexes have revealed coordinated olefins with bond distances of $1.345 (11) \text{ \AA}$ in $[(\text{C}_7\text{H}_8)\text{CuCl}]_4$,³² $1.366 (10) \text{ \AA}$ in $(\text{C}_7\text{H}_8)\text{PdCl}_2$,³³⁻³⁵ and $1.39 (5) \text{ \AA}$ in $(\text{C}_7\text{H}_8)(\text{AgNO}_3)_2$.³⁶ Other carbon-carbon distances within the present norbornadiene system are in the ranges

$\text{C}(\text{sp}^2)\text{-C}(\text{sp}^3) = 1.512 (9)\text{-}1.542 (8)$, and $\text{C}(\text{sp}^3)\text{-C}(\text{sp}^3) = 1.523 (9)\text{-}1.527 (10) \text{ \AA}$.

As shown by the torsional angles collected in Table VI, the norbornadiene ligand has close to ideal C_{2v}

Table VI. Torsional Angles^a within the Norbornadiene Fragment

Atoms	Angle (deg)	Atoms	Angle (deg)
C(1)-C(2)-C(3)-C(4)	1.15	C(5)-C(6)-C(1)-C(7)	32.53
C(2)-C(3)-C(4)-C(5)	69.51	C(2)-C(3)-C(4)-C(7)	34.88
C(3)-C(4)-C(5)-C(6)	70.03	C(6)-C(5)-C(4)-C(7)	34.22
C(4)-C(5)-C(6)-C(1)	1.13	C(1)-C(7)-C(4)-C(3)	127.74
C(5)-C(6)-C(1)-C(2)	71.27	C(1)-C(7)-C(4)-C(5)	129.17
C(6)-C(1)-C(2)-C(3)	71.84	C(4)-C(7)-C(1)-C(2)	128.79
C(3)-C(2)-C(1)-C(7)	33.01	C(4)-C(7)-C(1)-C(6)	129.48

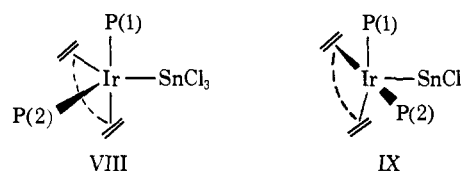
^a These are torsional angles about the middle bond.

symmetry. Bond angles within the carbon-atom framework of this ligand fall into three sets. The $\text{C}(\text{sp}^3)\text{-C}(\text{sp}^2)\text{-C}(\text{sp}^2)$ angles vary from $105.3 (5)$ to $106.1 (5)^\circ$, the C-C-C angles centered on C(1) and C(4) range from $98.7 (4)$ to $102.6 (6)^\circ$, and the angle at the bridging apex, *i.e.*, C(1)-C(7)-C(4), is $93.6 (5)^\circ$.

$\text{C}(\text{sp}^2)\text{-H}$ bond distances range from $0.81 (7)$ to $1.04 (6) \text{ \AA}$ (averaging 0.95 \AA), while the $\text{C}(\text{sp}^3)\text{-H}$ distances have values between $0.81 (7)$ and $1.03 (8)$, with a mean of 0.93 \AA . Angles involving hydrogen are all reasonable (see Table IV, section F).

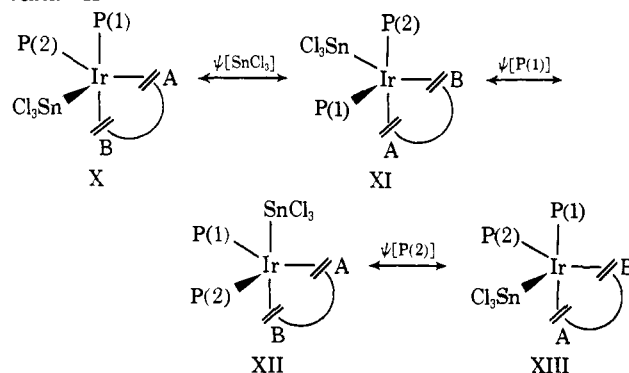
Conclusion

As pointed out above, the true coordination geometry about the central iridium(I) atom in $(\text{C}_7\text{H}_8)(\text{PMe}_2\text{Ph})_2\text{-Ir}(\text{SnCl}_3)$ is midway between the idealized trigonal bipyramidal (VIII) and square pyramidal (IX) representations.



Working within the framework of the trigonal bipyramidal formalism, equilibration of vinylic protons on the norbornadiene ligand may be explained in terms of Scheme II, which involves successive pseudoro-

Scheme II



tations about SnCl_3 [X \rightarrow XI], P(1) [XI \rightarrow XII], and P(2) [XII \rightarrow XIII].

The fact that the ground state of the molecule is distorted away from the idealized trigonal bipyramidal

(21) R. L. Livingston and C. N. R. Rao, *J. Chem. Phys.*, **30**, 339 (1959).

(22) P. T. Greene and R. F. Bryan, *J. Chem. Soc. A*, 1696 (1970).

(23) G. A. Melson, P. F. Stokely, and R. F. Bryan, *J. Chem. Soc. A*, 2247 (1970).

(24) L. Manojlovic-Muir, K. W. Muir, and J. A. Ibers, *Inorg. Chem.*, **9**, 447 (1970); see, especially, Table VI on p 452.

(25) R. F. Bryan, *J. Chem. Soc. A*, 172 (1967).

(26) R. F. Bryan, *J. Chem. Soc. A*, 192 (1967).

(27) H. P. Weber and R. F. Bryan, *Acta Crystallogr.*, **22**, 822 (1967).

(28) R. F. Bryan, *J. Chem. Soc. A*, 696 (1968).

(29) P. T. Greene and R. F. Bryan, *J. Chem. Soc. A*, 2261 (1970).

(30) J. F. Young, *Advan. Inorg. Chem. Radiochem.*, **11**, 91 (1968); see, especially, Table VI on p 130.

(31) H. A. Bent, *Chem. Rev.*, **61**, 275 (1961).

(32) N. C. Baenziger, H. L. Haight, and J. R. Doyle, *Inorg. Chem.*, **3**, 1535 (1964).

(33) N. C. Baenziger, G. F. Richards, and J. R. Doyle, *Acta Crystallogr.*, **18**, 924 (1965); this paper supercedes the previous reports (see ref 34 and 35) of this structure.

(34) N. C. Baenziger, J. R. Doyle, G. F. Richards, and C. L. Carpenter, "Advances in the Chemistry of the Coordination Compounds," Macmillan, New York, N. Y., 1961, pp 131-138.

(35) N. C. Baenziger, J. R. Doyle, and C. L. Carpenter, *Acta Crystallogr.*, **14**, 303 (1961).

(36) N. C. Baenziger, H. L. Haight, R. Alexander, and J. R. Doyle, *Inorg. Chem.*, **5**, 1399 (1966).

structure (X) toward a square pyramidal structure with SnCl_3 axial (*i.e.*, IX) simply means that the forward reaction in Scheme II commences at some stage intermediate between X and XI and terminates at some (symmetrically related) stage intermediate between XII and XIII; *i.e.*, the observed structure lies on the reaction coordinate of the idealized Berry pseudorotation process $\text{X} \rightarrow \text{XI}$.

In contrast to the case of (cycloocta-1,5-diene)(phosphine) $_2\text{Ir}(\text{CH}_3)$ species (see Scheme I, in the introduction), the rate-limiting step in the present equilibration of vinylic protons clearly occurs during the second pseudorotation (about P(1)), during which the strong π -acceptor ligand, SnCl_3 , is moved into the energetically unfavorable axial position. The energy required for this step clearly will decrease with increasing P(1)–Ir–P(2) angle, since it involves, *inter alia*, the transformation of phosphine ligands from an axial–equatorial pair (for which the idealized angle is 90°) to a diequatorial pair (for which the ideal interligand angle is 120°).

Our previous studies on (cycloocta-1,5-diene)(phosphine) $_2\text{Ir}(\text{CH}_3)$ species^{1–3} have shown the P–Ir–P angle to be $84.9(2)^\circ$ for $\text{P}(1)\widehat{\text{P}}(2) = \text{Ph}_2\text{P}(\text{CH}_2)_2\text{PPh}_2$, $93.4(1)^\circ$ for $\text{P}(1)\widehat{\text{P}}(2) = \text{Ph}_2\text{P}(\text{CH}_2)_3\text{PPh}_2$, and $101.5(2)^\circ$

for $\text{P}(1) = \text{P}(2) = \text{PMe}_2\text{Ph}$. It follows, therefore, that the energy required for equilibration of the vinylic diene protons in the trichlorostannatoiridium(I) species will vary as a function of phosphine ligand in the order $(\text{PMe}_2\text{Ph})_2 < \text{Ph}_2\text{P}(\text{CH}_2)_3\text{PPh}_2 < \text{Ph}_2\text{P}(\text{CH}_2)_2\text{PPh}_2$; *i.e.*, the effect of chelation and of chelate ring size is predicted (*as observed*^{4b}) to be precisely the opposite to that found in the *methyliridium*(I) systems.

Acknowledgments. We are grateful to Professor J. A. Osborn for providing the sample, for helpful discussions, and for his continuing interest in these studies. This work was made possible by a generous allocation of computer time on an IBM 370/155 at the Computer Center, University of Illinois at Chicago Circle, and by financial support from the National Science Foundation through Grant GP-33018 (to M. R. C.).

Supplementary Material Available. A listing of structure factor amplitudes will appear following these pages in the microfilm edition of this volume of the journal. Photocopies of the supplementary material from this paper only or microfiche (105×148 mm, $24\times$ reduction, negatives) containing all of the supplementary material for the papers in this issue may be obtained from the Journals Department, American Chemical Society, 1155 16th Street, N.W., Washington, D. C. 20036. Remit check or money order for \$4.00 for photocopy or \$2.00 for microfiche, referring to code number JACS-74-76.

Stereochemistry of Low-Spin Cobalt Porphyrins. III. The Crystal Structure and Molecular Stereochemistry of Bis(piperidine)- $\alpha,\beta,\gamma,\delta$ -tetraphenylporphinatocobalt(II)

W. Robert Scheidt

Contribution from the Department of Chemistry, University of Notre Dame,
Notre Dame, Indiana 46556. Received May 10, 1973

Abstract: Bis(piperidine)- $\alpha,\beta,\gamma,\delta$ -tetraphenylporphinatocobalt(II) crystallizes in the triclinic system, space group $P\bar{1}$. The unit cell has $a = 11.503(3) \text{ \AA}$, $b = 11.830(4) \text{ \AA}$, $c = 9.934(4) \text{ \AA}$, $\alpha = 101.99(2)^\circ$, $\beta = 115.64(2)^\circ$, $\gamma = 101.49(2)^\circ$ and contains one molecule. The calculated and experimental densities are 1.271 and 1.265 g/cm³, respectively, at $20 \pm 1^\circ$. Measurement of diffracted intensities employed θ - 2θ scans with graphite-monochromated Mo $K\alpha$ radiation on a Syntex four-circle diffractometer. All independent reflections for $(\sin \theta/\lambda) \leq 0.648 \text{ \AA}^{-1}$ were scanned; 4360 reflections were retained as observed. These data were employed for the determination of structure using the heavy-atom technique and anisotropic least-squares refinement of the 277 structural parameters. The final conventional and weighted discrepancy factors were 0.043 and 0.059, respectively. The octahedral CoN_6 coordination group in the centrosymmetric (C_i - $\bar{1}$) molecule approximates to full tetragonal symmetry. Equatorial bond lengths are 1.987 \AA with an esd for an individual determination of 0.002 \AA . The axial Co–N bond is extended to 2.436 (2) \AA and is attributable to the unpaired electron located principally in the d_{z^2} orbital. Bond distances and angles of any specified chemical class in the porphinato core display trivial departures from D_{4h} symmetry.

Our interest in the structural characterization of low-spin cobalt(II) porphyrins was prompted by Walker's¹ electron spin resonance (esr) studies of low-spin cobalt(II) porphyrins. She observed three distinctive classes of compounds in toluene glasses at 77°K . These involve the coordination by the cobalt(II) atom of (a) a single molecule of a nitrogen base, (b) two molecules of base, or (c) one molecule of base and one molecule of reversibly bound oxygen. A particu-

larly notable feature is the invariance of the esr parameters, within each class, with respect to large differences in the basicity, chemical constitution, and the steric requirements of the nitrogen base. Equally pertinent are the studies of Hoffman, *et al.*,^{2,3} on co-

(2) B. M. Hoffman and D. H. Petering, *Proc. Nat. Acad. Sci. U. S.*, 67, 637 (1970).

(3) (a) B. M. Hoffman, C. A. Spilburg, and D. H. Petering, *Cold Spring Harbor Symp. Quant. Biol.*, 36, 343 (1971); (b) C. A. Spilburg, C. Bull, and B. M. Hoffman, *Fed. Proc., Fed. Amer. Soc. Exp. Biol.*, 31, 484 (1972); (c) G. C. Hsu, C. A. Spilburg, C. Bull, and B. M. Hoffman, *Proc. Nat. Acad. Sci. U. S.*, 69, 2122 (1972).

(1) F. A. Walker, *J. Amer. Chem. Soc.*, 92, 4235 (1970).